



Luminescence and structural studies of yttrium and heavier lanthanide–picrate complexes with pentaethylene glycol

Eny Kusurini^{a,*}, Muhammad Idiris Saleh^{b,*}

^aDepartment of Chemical Sciences, Faculty of Science and Technology, Universiti Malaysia Terengganu, 21030 Kuala Terengganu, Terengganu, Malaysia

^bSchool of Chemical Sciences, Universiti Sains Malaysia, 11800 Penang, Malaysia

ARTICLE INFO

Article history:

Received 24 June 2008

Received in revised form 17 May 2009

Accepted 22 May 2009

Available online 29 May 2009

Keywords:

Heavier lanthanide
Pentaethylene glycol
Photoluminescence
X-ray crystal structures

ABSTRACT

The monoclinic structural isomers with molecular formula of $[M(\text{Pic})_2(\text{EO5})](\text{Pic})$ where EO5 = pentaethylene glycol, Pic = picrate anion, and M = Gd, Tb, Er, Tm, Yb, and Y have been synthesized and characterized. The current study was conducted in the solid state to evaluate the coordination pattern of the central metal ion with the EO5 ligand in the presence of Pic anion. The photoluminescence (PL) spectra of the Tb and Yb complexes have the typical 4f–4f transition emissions of Tb(III) and Yb(III) ions. The Gd, Er, Tm, and Y complexes had broad bands resulting from the ligands. The counteranion factor influenced the emission intensity in the Tb–Pic–EO5 and Tb–NO₃–EO5 complexes in several solvents also were studied. The Pic anion acts as a quencher in the $[\text{Tb}(\text{Pic})_2(\text{EO5})](\text{Pic})$ complex due to the nitro withdrawing groups was clearly observed both in solution and the solid state.

© 2009 Elsevier B.V. All rights reserved.

1. Introduction

The coordination behavior of lanthanide ion with the acyclic EO5 ligand has attracted interest due to the strong coordination capability with the metal ion, flexible structure and its donor oxygen atoms can be coordinated to the metal ion in a hexadentate mode effects for luminescence properties and their ability to adopt different structural diversity [1–5]. The picric acid (HPic) may displace the coordinated water molecule [4,6] as well as increase the molecular rigidity to attain the high efficiency luminescence property. Scheme 1a and b shows the molecular structure of the EO5 and HPic molecules [3].

In this article, we report the preparation, spectral characterization, molar conductance, luminescence, and crystal structures determination of the yttrium and heavier lanthanide complexes, $[M(\text{Pic})_2(\text{EO5})](\text{Pic})$. The nitro withdrawing group from the Pic anion plays an important role in modifying of the luminescence properties of the prepared compounds.

2. Experimental

2.1. Materials

All chemicals and solvents were of analytical grade and used without further purification. Pentaethylene glycol (EO5, C₁₀H₂₂O₆,

≥97% purity) was purchased from Fluka (Buchs, Switzerland). HPic ((NO₂)₃ C₆H₂OH, >98% purity) was purchased from BDH (Poole, England). M(NO₃)₃·5H₂O (99.9% purity) for M = Tb, Er, Tm, Yb, and Y were purchased from Aldrich (Wisconsin, USA). Gd(NO₃)₃·6H₂O (99.9% purity) was obtained from Johnson Matthey Electronic (New Jersey, USA).

2.2. Preparation of the complexes

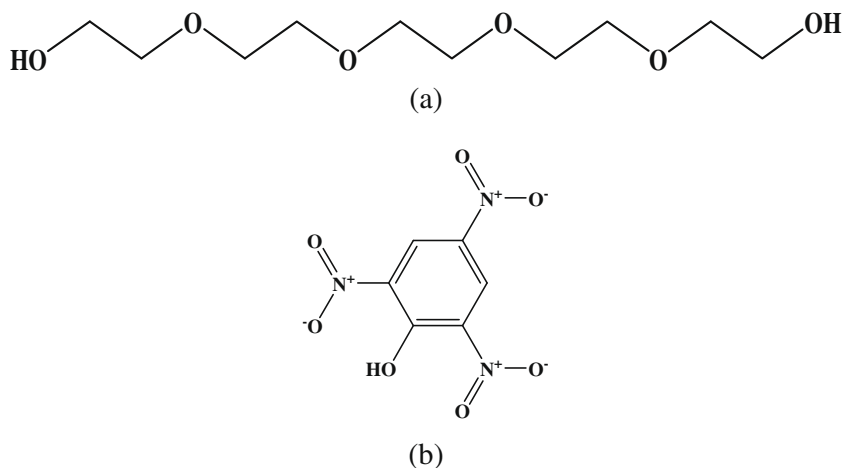
The complexes were prepared as previously described [1–5]. A mixture of EO5 (0.6 g, 2.52 mmol), HPic (0.91 g, 3.97 mmol), and $[M(\text{NO}_3)_3 \cdot 7\text{H}_2\text{O}]$ (0.434 g, 1 mmol) for each M = Gd, Tb, Er, Tm, Yb, and Y was dissolved in 20 mL acetonitrile:methanol (3:1, v/v). The solution mixture was stirred for 5 min. The mixture was left to stand for 1–5 days at room temperature and single crystals for Gd (60%), Tb (80%), Er (60%), and Y (75%) suitable for X-ray diffraction determination were collected. However, the reactions of EO5 and HPic with the Tm and Yb nitrate salts in acetonitrile:methanol (3:1, v/v) did not result in any single crystal products.

2.3. Physical measurements

The percentages of carbon, hydrogen, and nitrogen were determined by using a Perkin–Elmer 2400II elemental analyzer. Conductivity measurements were made in a DMSO solution at 25.95 ± 0.01 °C using a Scan500 conductivity meter. IR spectra were recorded on a Perkin–Elmer 2000 FTIR spectrophotometer in the region of 4000–400 cm⁻¹ by using the conventional KBr pellet method for solid samples. For liquid sample, e.g. the EO5 ligand,

* Corresponding authors. Tel.: +609 6683676; fax: +609 6683326.

E-mail addresses: e.kusurini@umt.edu.my (E. Kusurini), midiris@usm.my (M.I. Saleh).



Scheme 1.

a thin layer of sample was applied to the surface of a KRS-5 (thallium bromoiodide).

Photoluminescence (PL) measurements were made at room temperature by using a Jobin Yvon HR800UV system. The data were collected and processed with Labspec Version 4 software. An HeCd laser was used for excitation at 325 nm, and the emission spectra were scanned from 330 to 1000 nm. An incident laser (20 mW) was used as the excitation source. A microscope objective lens (UV40 \times) was used to focus the laser on the sample surface. The emitted light was dispersed by a double grating monochromator (0.8 m focal length) equipped with an 1800 groove/mm holographic plane grating. Signals were detected with a Peltier-cooled CCD4 array detector.

Fluorescence measurements were made with a Jasco Spectrofluorometer Model FP-750 at room temperature with a xenon light source, and the excitation and emission slits used were both 5 nm. The emission spectra were scanned from 220 to 730 nm at 500 nm/min. The concentrations for samples were 80 $\mu\text{mol/L}$.

2.4. X-ray crystallographic study

X-ray diffraction data were collected from single crystals by using a Bruker APEX2 area-detector diffractometer with a graphite monochromated Mo K α radiation source and a detector distance of 5 cm. Data were processed using APEX2 software [7]. The collected data were reduced by using the SAINT program and the empirical absorption corrections were applied with the SADABS program [7]. The structures were solved by direct methods and refined by least-squares method on F_{obs}^2 using the SHELXTL program [8]. All non-hydrogen atoms were refined anisotropically. Hydrogen atoms were located from different Fourier maps and were isotropically refined. The final refinement converged well. Data for publication were prepared with SHELXTL [8] and PLATON [9]. Crystallographic data and refinement of the $[\text{M}(\text{Pic})_2(\text{EO5})](\text{Pic})$ complexes are summarized in Table 1. Selected bond lengths, and bond angles of the complexes studies are listed in Table 2. One oxygen atom (O20) in the Gd complex is disordered over two positions with refined occupancies of

Table 1
Summary of crystallographic data and refinement for the $[\text{M}(\text{Pic})_2(\text{EO5})](\text{Pic})$ complexes.

Parameter	Compound			
	Gd	Tb	Er	Y
Formula	$\text{C}_{28}\text{H}_{28}\text{N}_9\text{O}_{27}\text{Gd}$	$\text{C}_{28}\text{H}_{28}\text{N}_9\text{O}_{27}\text{Tb}$	$\text{C}_{28}\text{H}_{28}\text{N}_9\text{O}_{28}\text{Er}$	$\text{C}_{28}\text{H}_{28}\text{N}_9\text{O}_{27}\text{Y}$
Formula weight	1079.84	1081.51	1089.85	1011.50
Volume (\AA^3)	3702.68(14)	3829.23(15)	3818.5(3)	3818.1(4)
Crystal system	monoclinic	monoclinic	monoclinic	monoclinic
Space group	$P2_1/c$	$P2_1/c$	$P2_1/c$	$P2_1/c$
Z	4	4	4	4
<i>Unit cell dimensions</i>				
a (\AA)	18.4972(4)	18.7250(3)	18.707(8)	18.708(1)
b (\AA)	8.9107(2)	8.9956(2)	8.980(4)	8.985(5)
c (\AA)	23.7748(5)	24.0786(7)	24.077(1)	24.063(1)
$\alpha = \gamma$ ($^\circ$)	90	90	90	90
β ($^\circ$)	109.1100(10)	109.2440(10)	109.252(1)	109.272(1)
D_{calc} (g/cm^3)	1.937	1.876	1.896	1.760
μ (mm^{-1})	1.911	1.963	2.314	1.644
$F(0\ 0\ 0)$	2156	2160	2172	2056
Crystal size (mm)	$0.50 \times 0.39 \times 0.11$	$0.43 \times 0.30 \times 0.25$	$0.50 \times 0.34 \times 0.34$	$0.24 \times 0.20 \times 0.20$
θ Range ($^\circ$)	1.17–30.00	1.15–26.41	2.41–28.29	2.41–28.28
h, k, l	26/–25, –12/12, –33/33	0/23, 0/12, –31/30	–24/21, –11/11, –20/31	–24/24, –11/11, –31/22
Reflections collected/unique (R_{int})	112 256/10 805 (0.0473)	7620/7620 (0.0000)	22 884/9329 (0.021)	23 312/9310 (0.037)
Data/restraints/parameter	10 805/3/598	6187/0/586	9329/0/586	9437/0/596
Final R indices [$I > 2\sigma(I)$]	$R_1 = 0.0502$, $wR_2 = 0.1259$	$R_1 = 0.0512$, $wR_2 = 0.1291$	$R_1 = 0.0322$, $wR_2 = 0.081$	$R_1 = 0.054$, $wR_2 = 0.148$
R indices (all data)	$R_1 = 0.0540$, $wR_2 = 0.1317$	$R_1 = 0.0720$, $wR_2 = 0.1656$	$R_1 = 0.040$, $wR_2 = 0.086$	$R_1 = 0.087$, $wR_2 = 0.175$
Goodness-of-fit	1.213	1.184	1.071	1.036

Table 2
Selected bond lengths (Å) and bond angles (°) in the [M(Pic)₂(EO5)](Pic) complexes.

Bond	Length (Å)				Bond	Angle (°)			
	Gd	Tb	Er	Y		Gd	Tb	Er	Y
M1–O1	2.479(3)	2.441(4)	2.419(2)	2.414(3)	O1–M1–O2	63.88(9)	62.72(15)	63.1(9)	63.2(1)
M1–O2	2.541(3)	2.530(5)	2.507(3)	2.506(3)	O3–M1–O2	61.59(10)	62.16(18)	62.9(1)	62.9(1)
M1–O3	2.438(3)	2.511(4)	2.478(3)	2.483(3)	O3–M1–O4	63.42(10)	63.68(17)	63.3(1)	63.2(1)
M1–O4	2.515(3)	2.443(4)	2.424(3)	2.428(3)	O4–M1–O5	62.67(11)	61.82(14)	61.9(9)	61.9(1)
M1–O5	2.528(4)	2.527(4)	2.510(2)	2.509(3)	O6–M1–O5	63.03(11)	63.37(13)	63.7(8)	63.8(9)
M1–O6	2.441(3)	2.476(4)	2.450(2)	2.451(3)	O1–M1–O6	71.30(10)	72.0(1)	71.9(8)	71.8(9)
M1–O7	2.302(3)	2.296(4)	2.270(2)	2.262(3)					
M1–O14	2.308(3)	2.288(4)	2.268(2)	2.259(3)					
M1–O8	2.476(3)	2.484(4)	2.445(3)	2.451(3)					

71:29. Four oxygen atoms (O20, O23, O25, and O26) in the Tb complex are disordered over two positions with refined occupancies of 77:23, 75:25, 73:27, and 44:66.

3. Results and discussion

3.1. Physical properties and spectral analysis

Analytical data for the newly synthesized complexes indicate that the complexes are consistent with a 1:1:3 (metal-to-ligand-to-picric acid) compositions, [M(Pic)₂(EO5)](Pic) (Table 3). For comparison studies, these complexes can be formed following by slow evaporation in THF, CH₃CN, CH₃OH, and H₂O solutions within a relatively short time (few days). However, the complex can be obtained in the DMSO solution after slow evaporation for a long time (seven months). This slow formation is due to the tight competition between the coordination oxygen donor atoms from the DMSO molecule and the Pic anion.

The solubility of the complexes in common solvents is low, which made solution studies difficult and prevented the measurement of conductivity [5,6]. Conductivity measurement has provided a method of testing the degree of ionization of the complexes, the molecular ion that a complex liberates in solution, the higher will be its molar conductivity and vice versa [10]. The molar conductivity values for the [M(Pic)₂(EO5)](Pic) complexes were in the range 113–189 Ω⁻¹ mol⁻¹ cm³ indicating that the complexes to be electrolytes nature in a 1:3 ratio [5] (Table 3). This means that the DMSO molecules have replaced the two Pic anions from the structures of cation in solution. Thus, the actual solution species that is the [M(DMSO)₃(EO5)]³⁺ and three Pic anions. From this results are in a well agreement and prove the suggested that the formation of [M(Pic)₂(EO5)](Pic) complexes in DMSO solution is slowly.

Upon complexation, the typically absorption stretching bands of ν(O–H), ν(C–H), ν(C–C), ν(C–O–C), ν₃(NO₂), ν₂(NO₂), and ν(C–N) were shifted towards the free EO5 and HPic molecules. On the basis of the similarity of their IR spectra, we assume that the complexes studied have similar structures with the lighter lanthanide EO5 complexes have been reported by Saleh et al. [1–4] and Kusriani et al. [5]. The IR spectra of the complexes had broad bands over

3400 cm⁻¹ that may be attributed to O–H...O hydrogen bonding [5].

3.2. X-ray studies

The structural isomers of [M(Pic)₂(EO5)](Pic) complexes are crystallized in a monoclinic with space group *P*2₁/*c* (Table 1). The volume of the complexes is reduced due to the heavier lanthanide ions. The Y complex is like the heavier lanthanide complexes. The lighter and heavier lanthanide ions control the geometry of the inner coordination spheres in the Ln–picric acid complexes [6]. The calculated density of the Y complex is the smallest (1.760 g/cm³). Meanwhile, the calculated density of the Gd complex is the highest (1.937 g/cm³), thus suggesting that the crystal packing in the Gd complex is more efficient than that in the Er, Tb, and Y complexes.

The asymmetric unit of the complexes studied, contain two crystallographically independent [M(Pic)₂(EO5)]⁺ and a Pic anion. The most favorable site of the Pic anion is the negatively charged phenolic oxygen due to the ion–ion interaction [11]. The oxygen atom of *ortho*-nitro group is also favorable coordination site due to the charge localization on this oxygen atom. Between the phenolic and *ortho*-nitro oxygen atoms had the short distance about of 2.683 Å that provide an effective bidentate mode with both charge and dipole binding ability [12].

The central metal ion was coordinated to nine donor oxygen atoms and the positive charge was balanced by one Pic anion acts as a counteranion. Six oxygen atoms belong to the EO5 ligand in hexadentate mode and the remaining three from each bidentate and monodentate Pic anions (Fig. 1). The slightly distorted tricapped trigonal prismatic geometry has the O1, O3, and O5 atoms at the peak of the capping position of the three square planes for the Tb, Er, and Y complexes. The oxygen atoms as a peak of the capping position, namely O1, O3, and O5 form the trigonal plane which is the Tb1, Er1, and Y1 atoms lie on the center of this trigonal plane (Fig. 2). Because of the O1, O3, and O5 atoms are coplanar with the central metal ion with maximum deviation of –0.004(1) Å for the Tb1 atom, –0.001(1) Å for the Er1 atom, and 0.000(4) Å for the O3 atom. As in the other EO5 complexes, the inner coordination sphere of [Gd(Pic)₂(EO5)]⁺ has a slightly tricapped trigonal prismatic geometry with the O2, O4, and O6 atoms coplanar and

Table 3
Elemental analysis of the [M(Pic)₂(EO5)](Pic) complexes.

Compound	Decomposition (°C)	Found (Calc.) (%)			Yield	molar conductivity (Ω ⁻¹ mol ⁻¹ cm ³)	Colour
		C	H	N			
Gd	260.5–276.8	31.23 (31.04)	2.47 (2.52)	11.64 (11.69)	60	182	yellow
Tb	254.4–273.1	31.17 (31.01)	2.57 (2.51)	11.66 (11.62)	80	125	yellow
Er	237.6–256.2	30.84 (30.74)	2.61 (2.47)	10.97 (11.53)	60	139	yellow
Tm	148.6–229.7	29.82 (30.71)	2.26 (2.56)	11.66 (11.52)	50	189	yellow
Yb	226.0–243.9	29.82 (30.69)	2.26 (2.55)	11.66 (11.50)	40	113	yellow
Y	247.5–256.0	33.06 (33.13)	2.78 (2.86)	12.17 (12.42)	75	113	Yellow

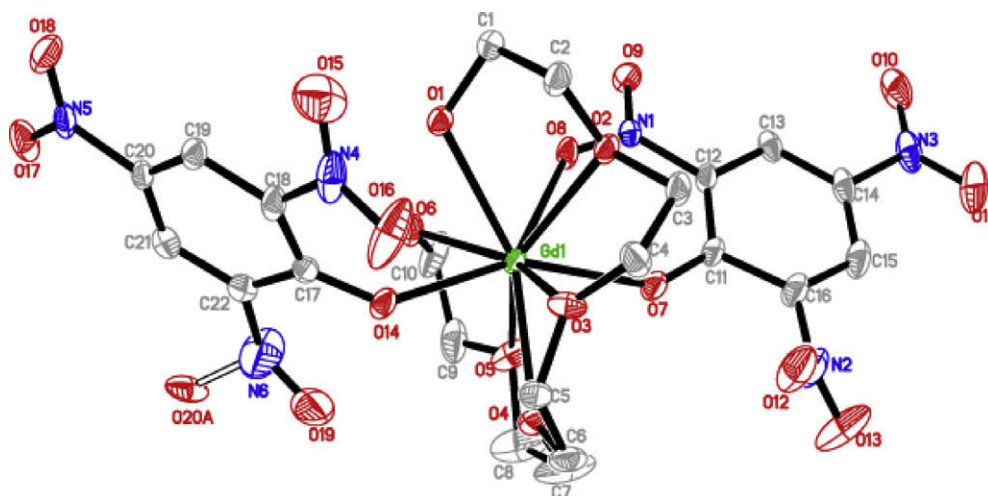


Fig. 1. Molecular structure of $[\text{Gd}(\text{Pic})_2(\text{EO5})](\text{Pic})$ complex with 50% probability ellipsoids. All the hydrogen atoms and the Pic counteranion have been omitted for clarity.

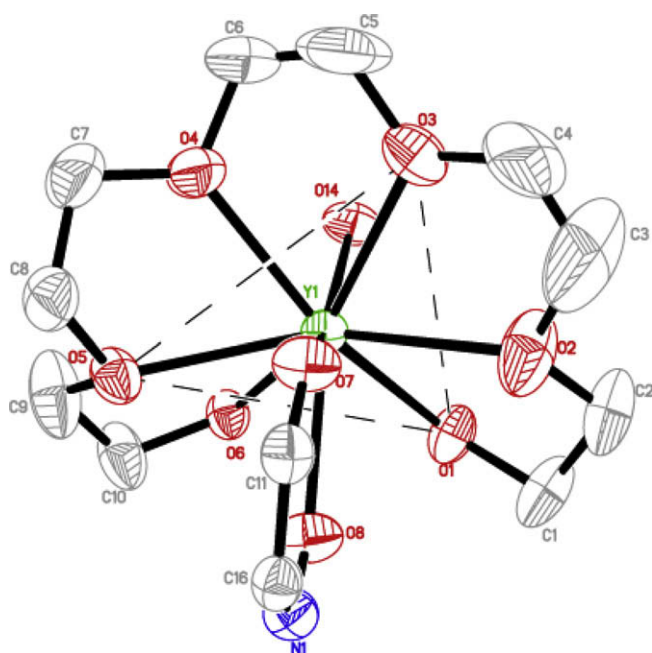


Fig. 2. The inner coordination sphere of $[\text{Y}(\text{Pic})_2(\text{EO5})]^+$ shows the trigonal plane from the O1–O3–O5 atoms.

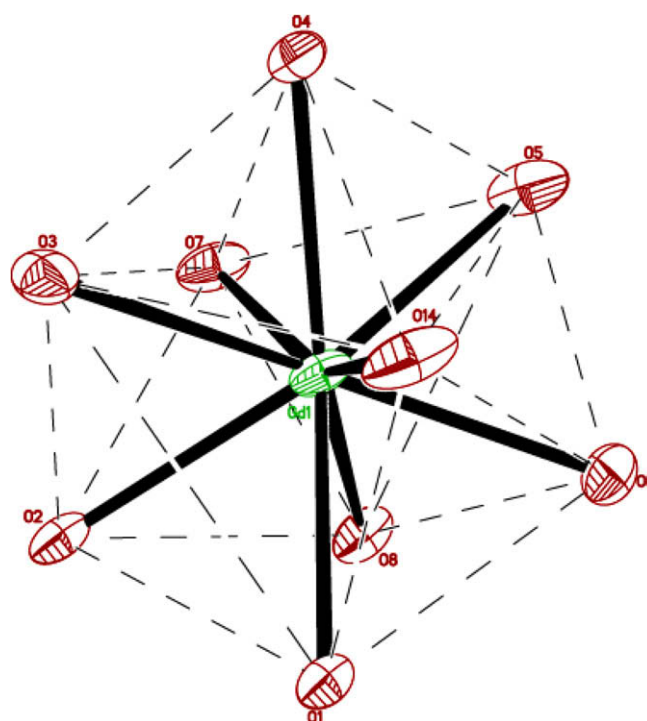


Fig. 3. Coordination geometry around the Gd1 atom as a tricapped trigonal prismatic.

at the top in the capping position (Fig. 3). The Gd1 atom also lies on the trigonal plane from the O2–O4–O6 atoms. This is due the O2, O4, and O6 atoms are coplanar with the Gd1 atom with maximum deviation of $-0.001(1)$ Å for the Gd1 atom.

Both aromatic rings of the coordinated Pic anions were planar and made dihedral angles with the structures of cation, i.e. $88.03(18)^\circ$, $89.3(2)^\circ$, $89.2(2)^\circ$, and $89.4(2)^\circ$ for the Gd, Tb, Er, and Y complexes, respectively. Fig. 2 shows the acyclic EO5 ligand was coordinated to the central metal ion in the complexes which exhibited pseudo-cyclic behavior [1–5]. The Pic anion can prevent the water molecules involved in the inner coordination sphere of these compounds was clearly observed.

All of the M–O bond lengths were reduced from the Gd, Tb, Er, and Y complexes with respect to increasing of the atomic number or lanthanide contraction effect (Table 2). The effective ionic radii of Gd(III), Tb(III), Er(III), and Y(III) ions were quite similar, i.e. 1.107, 1.095, 1.062, and 1.075 Å, respectively [13]. In this case a

nine-coordination number was found [13]. The $\text{M}-\text{O}_{\text{ether}}$ bond lengths are longer than the $\text{M}-\text{O}_{\text{alcohol}}$ bond lengths. The average $\text{M}-\text{O}_{\text{phenol}}$ bond lengths are the shortest, i.e. 2.305(3), 2.292(4), 2.269(2), and 2.261(3) Å, respectively, for the Gd, Tb, Er, and Y complexes. The shorter of bond length is caused by the higher electron density of the phenolic oxygen of the Pic anion [1–6,14]. The $\text{M}-\text{O}_{\text{nitro}}$ bond length for the heavier lanthanide–picrate complexes is shorter than those found in the lighter lanthanide–picrate complexes [1–5]. These lengths are influenced by the free position of the *ortho*-nitro oxygen atoms before this oxygen is coordinated with the metal ion. In the Gd complex, both of the nitro groups of the bidentate Pic anion are rotated with respect to the aromatic part with torsion angles of $\text{O8}-\text{N1}-\text{C12}-\text{C11}$ [$4.4(6)^\circ$]; $\text{O9}-\text{N1}-\text{C12}-\text{C11}$ [$-174.7(4)^\circ$] and $\text{O12}-\text{N2}-\text{C16}-\text{C11}$ [$-49.8(7)^\circ$]; $\text{O13}-\text{N2}-\text{C16}-\text{C11}$ [$130.9(6)^\circ$]. While, both of the nitro groups of the monodentate Pic anion also are rotated with respect to the aro-

matic part with torsion angles of O12–N2–C16–C11 [$-49.8(7)^\circ$]; O13–N2–C16–C11 [$130.9(6)^\circ$] and O19–N6–C22–C17 [$20.0(11)^\circ$]; O20A–N6–C22–C17 [$148.2(7)^\circ$]. For the Tb, Er, and Y complexes, the behavior of the nitro groups of the coordinated Pic anion also are similar to those in the Gd complex. These values are comparable to those reported in the acid [15].

The O–M–O bond angle between the adjacent oxygen atoms in the inner coordination sphere of all of the complexes was approximately the same, and slightly larger than 60° (Table 2). The O6–M1–O1 bond angles in the heavier lanthanide complexes were slightly larger than the O6–M1–O1 bond angles in the lighter lanthanide complex [1–5]. The Tb, Er, and Y complexes showed the same a geometric conformational pattern in the EO5 ligand of $g^+ g^- g^+ g^-$ with following average O–C–C–O torsion angles of $40.06(8)^\circ$, $37.3(8)^\circ$, and $37.0(9)^\circ$, respectively. The Gd complex showed the geometric conformational pattern in the EO5 ligand of $g^+ g^+ g^- g^+ g^-$ with average torsion angle of $48.48(5)^\circ$. The O–C–C–O torsion angle patterns in the yttrium and heavier lanthanide complexes were different from those measured in the other derivative complexes involving La [4], Pr [1], Sm, and Dy [3]. Among the different lanthanide ion complexes, the structures of cation, and geometrical arrangement also influence the torsion angle sequence. All the C–O–C–C torsion angles are *anti*, except C2–O2–C3–C4 (for the Gd complex) and C9–O5–C8–C7 (for the Tb, Er, and Y complexes) is close to the *gauche* conformation (g^-).

There are different types of hydrogen bonding in the complexes that give rise to different supramolecular architectures. The complexes show one-dimensional (1D) architecture with symmetry direction [001] that is connected through intra- and intermolecular O–H...O and C–H...O hydrogen bonding (Fig. 4). The presence of the terminal alcoholic group provides the possibility of the formation of strong and weak hydrogen bonds to confer high stability on the Tb, Er, and Y complexes. However, both the terminal alcoholic groups only contribute to form the weak intra- and intermolecular hydrogen bonds were observed in the Gd complex (S1). The O–H...O, O–H...N, and C–H...O hydrogen bonds have stabilized in the crystal packing of the Gd complex. Only intermolecular O–H...O and C–H...O hydrogen bonds were stabilized the crystal packing of the Tb complex. Two bifurcated hydrogen bonds were observed for the Tb, Er, and Y complexes namely O6–H6C...O21 and O6–H6C...O27 and C8–H8A...O26 and C8–H8B...O7. The Pic counteranion is linked with $[M(\text{Pic})_2(\text{EO5})]^+$ by two weak hydrogen bonds, i.e. N8C–O25C...H13C–C13C [2.553 \AA] and C27–H27C...O10C–N2C [2.424 \AA], and then with the other adjacent

molecule units by N9C–O26C...H8AB–C8B [2.572 \AA] were observed in the Tb, Er, and Y complexes (Fig. 4).

The intermolecular π – π interactions between the Pic counteranion and the monodentate Pic anion via face-to-face mode with a centroid distance of 4.458(2), 4.484(3), 4.482(2), and 4.485(3) \AA , respectively, were observed in the Gd, Tb, Er, and Y complexes. The relative orientation of the two adjacent aromatic rings of the Pic anion is determined by the electrostatic repulsions between the two negatively charged π -systems

3.3. Photoluminescence (PL) studies

The ability of the EO5 and Pic ligands to satisfy the coordination requirements of the central Ln(III) with a high coordination number is an important criterion in the design of supramolecular photonic devices. However, the EO5 ligand also contains two terminal alcohol groups that may quench the lanthanide luminescence. The efficient non-radiative deactivations of the O–H and C–H groups, enables their participation in vibronic coupling with the vibrational state of the O–H and C–H oscillator [16]. The electron-withdrawing nitro and phenolic groups in the Pic ligand also influence the distribution of π -electronic density.

From the PL spectrum at room temperature, the HPic ligand had a broad emission band with the center peak at 537 nm ($18\,622 \text{ cm}^{-1}$) based on D2 filter measurement. The weak band assigned to the nitro group by n – π^* transition with an admixture of intra-ligand charge transfer (ILCT) is seen in the region of 350–425 nm. At excitation in transitions of aromatic anions and in the short-wavelength Ln(III) transitions the absorbed energy is transferred to the excited state of the nitro group. The direct excitation of the NO_2 group through n – π^* transition also occurs. The excitation energy can be dissipated in the lattice, transferred to the lowest excited ligand triplet level, where it can generate ligand fluorescence and Ln(III) luminescence. A dissipation channel for the excitation energy through the excited state of the NO_2 group from the Pic anion by π^* – n transition with participation of ILCT occurs in the Tb complex.

The free EO5 ligand had also broad emission bands with the highest intensity at 492.8 nm based on D2 filter measurements. The lowest triplet state energy level of the EO5 ligand [$T_1(\text{L})$] is $\sim 20\,292 \text{ cm}^{-1}$. This energy level is above the lowest excited resonance level $^5\text{D}_4$ ($\sim 20\,500 \text{ cm}^{-1}$) of Tb(III), but lower than the $^2\text{F}_{5/2}$ ($\sim 10\,300 \text{ cm}^{-1}$). The $T_1(\text{L})$ should be nearly equal to or lie above a resonance level of the central ion concerned. If the Ln(III) ion is

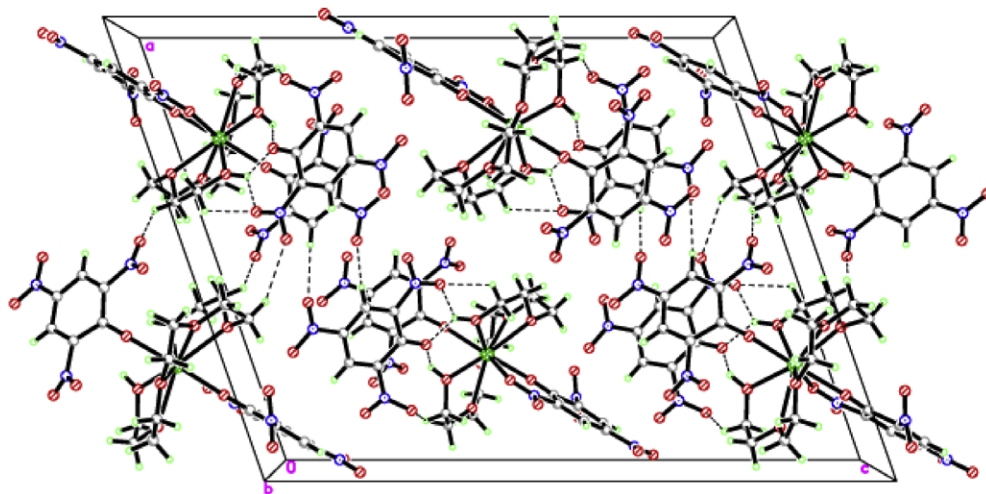


Fig. 4. View of the packing arrangement of the $[\text{Er}(\text{Pic})_2(\text{EO5})](\text{Pic})$ complex along *b*-axis. The hydrogen bonds are indicated by dashed lines.

excited by transfer of energy from the excited chelate molecule to the central ion resulting in line emission. Of the six complexes examined, only the Tb and Yb complexes have the typical 4f–4f transition emissions of Tb(III) and Yb(III). The PL spectra of the Gd, Er, Tm, and Y complexes had broad bands with the center peak at 535 nm due to the EO5 and Pic ligands. For the Gd complex, the metal-centered 4f–4f states are located at high energy about 313 nm, outside the visible spectral region due to the stability of the half-filled 4f⁷ shell configuration in the Gd(III) ion.

The $T_1(L)$ of the EO5 ligand is nearly equal with the lowest excited resonance level of Tb(III), therefore the intramolecular energy transfer is quite efficient and the emission intensity is increased. In the Tb complex, energy is primarily transferred from ligand triplet to the 5D_4 level from which luminescent transition to the ground state manifold 7F_J ($J = 0, 2, 3, 4, 5, 6$) are observed in the green spectral region (Table 4). The most intense transition for Tb(III) is the $^5D_4 \rightarrow ^7F_5$ transition, corresponding to a green emission band at 542.9 nm. The $^5D_4 \rightarrow ^7F_5$ transition is magnet dipole and is less affected by environment than the $^5D_4 \rightarrow ^7F_6$ transition. In the solid state, the hypersensitive peak of the $^5D_4 \rightarrow ^7F_5$ transition for the Tb complex [542.6 nm; 4749×10^2 a.u.] is higher than that found in Tb(NO₃)₃·6H₂O [541.4 nm; 298.7×10^2 a.u.] and Tb₄O₇ [542.1 nm; 41.1×10^2 a.u.] [6].

The Yb complex has one weak peak emission at 978.2 nm with an emission intensity of ~220 a.u. that is assigned to the $^2F_{5/2} \rightarrow ^2F_{7/2}$ transition in the near infrared (NIR). The electron configuration of 4f¹³ for the Yb(III) ion only allows only the ground state of $^2F_{7/2}$ level and the excited state of $^2F_{5/2}$ level [17]. Due to the energy gap between the lowest triplet state energy level of the EO5 and Pic ligands, the lowest excited resonance level of the Yb(III) ion is very large. Thus, the energy could not be transferred from the $T_1(L)$ to the Yb(III) ion. The broad lines due to structural disorder and coordinated terminal alcohol groups were observed in the Tb and Yb complexes [2].

For further study, we prepared the Tb complex with the EO5 ligand in the presence of the nitrate anion. The crystal structure of the [Tb(NO₃)₂(EO5)](NO₃) complex has been reported by Roger et al. [18], but not its luminescence property. We studied luminescence properties of the [Tb(NO₃)₂(EO5)](NO₃) complex relative to the [Tb(Pic)₂(EO5)](Pic) complex in various solvents at an excitation wavelength of 275 nm (Table 4). The crystal solid of the [Tb(Pic)₂(EO5)](Pic) complex in DMSO solution had three peaks at 488, 549, and 615 nm. However, the [Tb(Pic)₂(EO5)](Pic) complex from direct mixtures of the EO5 ligand, terbium nitrate salt and HPic in each CH₃CN, CH₃OH, THF, and H₂O solution had only two broad weak peaks at 486 and 547 nm.

The [Tb(NO₃)₂(EO5)](NO₃) complex in CH₃CN and DMSO solution have the sharp typical emission peaks corresponding to the $^5D_4 \rightarrow ^7F_6$ (491 nm), $^5D_4 \rightarrow ^7F_5$ (541 nm), $^5D_4 \rightarrow ^7F_4$ (585 nm), and $^5D_4 \rightarrow ^7F_3$ (617 nm) transitions. These peaks may result from: (i) the symmetry alteration of Tb(III) in the complex, (ii) the rigid structure of the complex formed by two nitrate anions and one

of the EO5 ligand surrounding the Tb(III), or (iii) the equivalent distances between the Tb(III) ion and the donor oxygen atoms. In CH₃CN solution, the [Tb(NO₃)₂(EO5)](NO₃) complex has the strongest fluorescence followed by CH₃OH, DMSO, H₂O and THF. This order suggests that the coordinating effects of the solvent in the formation of complexes, i.e. solvent effect where vibrational quenching of the complexes excited state may occur through a high energy oscillator on the solvent molecule [16,19,20]. For the [Tb(NO₃)₂(EO5)](NO₃) complex, the broad band due to the $^5D_4 \rightarrow ^7F_3$ transition also was observed in H₂O, THF, and CH₃OH solution. That the Pic anion acts as a quencher in the [Tb(Pic)₂(EO5)](Pic) complex due to the nitro withdrawing groups was clearly observed both in solution and the solid state. In addition, the [Tb(Pic)₂(EO5)](Pic) complex is not suitable for organic light emitting diode devices because of its ionic character and low volatility.

4. Conclusion

The structural isomers [M(Pic)₂(EO5)](Pic) complexes were crystallized in monoclinic with space group $P2_1/c$. The central metal ion had nine-coordinates with six oxygen atoms from the EO5 ligand and three oxygen atoms from the two Pic anions. The Tb and Yb complexes have the typical 4f–4f emission transitions corresponding to the Tb(III) and Yb(III) ions. The Tb complex is not suitable for organic light emitting diode devices because of its ionic character and low volatility.

Acknowledgements

We thank the Malaysian Government for funding research grants FRGS and SAGA to support this research.

Appendix A. Supplementary material

Supplementary data associated with this article can be found, in the online version, at doi:10.1016/j.ica.2009.05.045.

References

- [1] M.I. Saleh, E. Kusrini, R. Adnan, I.A. Rahman, B. Saad, A. Usman, H.-K. Fun, B.M. Yamin, J. Chem. Crystallogr. 35 (2005) 469.
- [2] M.I. Saleh, E. Kusrini, B. Saad, R. Adnan, A.S. Mohamed, B.M. Yamin, J. Lumin. 126 (2007) 871.
- [3] M.I. Saleh, E. Kusrini, R. Adnan, B. Saad, B.M. Yamin, H.-K. Fun, J. Mol. Struct. 837 (2007) 169.
- [4] M.I. Saleh, E. Kusrini, B. Saad, H.-K. Fun, B.M. Yamin, J. Alloys Compd. 474 (2009) 428.
- [5] E. Kusrini, M.I. Saleh, E. Lacomte, Spectrochim. Acta Part A, 2009, in press.
- [6] M.I. Saleh, E. Kusrini, H.-K. Fun, B.M. Yamin, J. Organomet. Chem. 693 (2008) 2561.
- [7] Bruker, APEX2, SAINT and SADABS, Bruker AXS Inc., Madison, Wisconsin, USA, 2005.
- [8] G.M. Sheldrick, SHELXL V5.1, Bruker AXS Inc., Madison, Wisconsin, USA, 1998.
- [9] A.L. Spek, J. Appl. Crystallogr. 36 (2003) 7.
- [10] M.S. Refat, J. Mol. Struct. 842 (2007) 24.
- [11] U. Olsher, R.M. Izatt, J.B. Bradshaw, N.K. Dalley, Chem. Rev. 91 (1991) 137.
- [12] U. Olsher, F. Feinberg, F. Frolow, G. Shohum, Pure Appl. Chem. 68 (1996) 1195.
- [13] R.D. Shannon, Acta Crystallogr., Sect. A 32 (1976) 751.
- [14] L. Fan, W. Liu, X. Gan, N. Tang, M. Tan, W. Jiang, K. Yu, Polyhedron 19 (2000) 779.
- [15] M.I. Saleh, E. Kusrini, M.R. Mustaqim, H.-K. Fun, Acta Crystallogr., Sect. E 64 (2008) o1318.
- [16] N. Sabbatini, M. Guardigli, J.-M. Lehn, Coord. Chem. Rev. 123 (1993) 201.
- [17] M.H.V. Werts, J.W. Verhoeven, J.W. Hofstra, J. Chem. Soc., Perkin Trans. (2000) 433.
- [18] R.D. Rogers, J. Zhang, C.B. Bauer, J. Alloys Compd. 249 (1997) 41.
- [19] H.Q. Liu, T.C. Cheung, C.M. Che, Chem. Commun. (1996) 1039.
- [20] Y.-L. Guo, W. Dou, Y.-W. Wang, W.-S. Liu, D.-Q. Wang, Polyhedron 26 (2007) 1699.

Table 4

The photoluminescence data of the [Tb(Pic)₂(EO5)](Pic) complex in the solid state.

Compound	λ (nm)	Intensity $\times 10^2$ (a.u.)
Ligand region	414.7	1123
$^5D_4 \rightarrow ^7F_6$	493.1	2873.6
$^5D_4 \rightarrow ^7F_5$	542.9	4692
$^5D_4 \rightarrow ^7F_4$	584.3	2335
$^5D_4 \rightarrow ^7F_3$	620.4	1350
$^5D_4 \rightarrow ^7F_2$	645.5	841
$^5D_4 \rightarrow ^7F_0$	687.1	468